Chronic ER stress promotes cGAS/mtDNA-induced autoimmunity via ATF6 in myotonic dystrophy type 2

Claudia Günther (Claudia.Guenther@ukdd.de)
Technische Universität Dresden, Department of Dermatology

Sarah Rösing
Department of Dermatology, University Hospital Carl Gustav Carus, TU Dresden

Fabian Ullrich
University Hospital Bonn, Institute of Clinical Chemistry and Clinical Pharmacology, Institute of Experimental Haematology and Transfusion Medicine

Susann Meisterfeld
Department of Dermatology, University Hospital Carl Gustav Carus, TU Dresden

Franziska Schmidt
Department of Dermatology, University Hospital Carl Gustav Carus, TU Dresden

Nadia Eberl
Department of Dermatology, University Hospital Carl Gustav Carus, TU Dresden

Julia Wegner
Institute of Clinical Chemistry and Clinical Pharmacology, University Hospital Bonn

Martin Schlee
University Hospital Bonn https://orcid.org/0000-0003-3671-7639

Anja Wieland
Institute of Clinical Chemistry and Clinical Pharmacology, University Hospital Bonn

Daniel Hilbig
Department of Oncology, Hematology, Rheumatology and Immune-Oncology, University Hospital Bonn

Ulrike Reuner
Department of Neurology, University Hospital Carl Gustav Carus

Peter Mirtschink
Institute for Clinical Chemistry and Laboratory Medicine, Faculty of Medicine, TU Dresden

Stephan Drukewitz
Core Unit for Molecular Tumor Diagnostics (CMTD), National Center for Tumor Diseases (NCT), Partner Site Dresden, Institute of Human Genetics, University of Leipzig Medical Center

Alexander Rapp
TU Darmstadt https://orcid.org/0000-0001-9108-3929

Thomas Zillinger

Institute of Clinical Chemistry and Clinical Pharmacology, University Hospital Bonn

Stefan Beissert

Department of Dermatology, University Hospital Carl Gustav Carus, TU Dresden

Katrin Paeschke

Department of Oncology, Hematology, Rheumatology and Immune-Oncology, University Hospital Bonn

Gunther Hartmann

https://orcid.org/0000-0003-1021-2018

Eva Bartok

University Hospital, University of Bonn https://orcid.org/0000-0003-0556-1950

Article

Keywords: ER stress, ATF6, Autoimmunity, type I IFN, repeat expansions

Posted Date: June 28th, 2022

DOI: https://doi.org/10.21203/rs.3.rs-1784722/v1

Chronic ER stress promotes cGAS/mtDNA-induced autoimmunity via ATF6 in myotonic dystrophy type 2

Sarah Rösing[1], Fabian Ullrich[2,3], Susann Meisterfeld[1], Franziska Schmidt[1], Nadia Eberl[1], Julia Wegner[2], Martin Schlee[2], Anja Wieland[2], Daniel Hilbig[4], Ulrike Reuner[5], Peter Mirtschink[6], Stephan Drukewitz[7], Alexander Rapp[8], Thomas Zillinger[2], Stefan Beissert[1], Katrin Paeschke[4], Gunther Hartmann[2], Eva Bartok[2,3,9*], Claudia Günther[1*]

[1]Department of Dermatology, University Hospital Carl Gustav Carus, TU Dresden, 01307 Dresden, Germany

[2]Institute of Clinical Chemistry and Clinical Pharmacology, University Hospital Bonn, 53127 Bonn, Germany

[3]Institute of Experimental Haematology and Transfusion Medicine, University Hospital Bonn, 53127 Bonn, Germany

[4]Department of Oncology, Hematology, Rheumatology and Immune-Oncology, University Hospital Bonn, 53127, Bonn, Germany

[5]Department of Neurology, University Hospital Carl Gustav Carus, TU Dresden, 01307 Dresden, Germany

[6]Institute for Clinical Chemistry and Laboratory Medicine, Faculty of Medicine, TU Dresden, 01307 Dresden, Germany

[7]Core Unit for Molecular Tumor Diagnostics (CMTD), National Center for Tumor Diseases (NCT), Partner Site Dresden, Institute of Human Genetics, University of Leipzig Medical Center, Leipzig, Germany

[8]Department of Biology, Cell biology and Epigenetic, Technical University of Darmstadt, Darmstadt, Germany

[9]Unit of Experimental Immunology, Department of Biomedical Sciences, Institute of Tropical Medicine, Antwerp, Belgium

*equal contribution

Address correspondence to: Claudia Günther, Department of Dermatology, Medizinische Fakultät Carl Gustav Carus, Technische Universität Dresden, Fetscherstr. 74, 01307 Dresden, Germany. Phone: 0049.351.458 2344; E-mail: claudia.guenther@ukdd.de

Abstract

Nucleic acid accumulation in repeat expansion disease poses multiple challenges to cellular integrity. Myotonic dystrophy type 2 (DM2) results from large CCTG repeats in the CNBP gene leading to myopathy and an increased prevalence of autoimmunity. Here, we observed that DM2 patients exhibited a type-I interferon signature in blood and cultured fibroblasts. RNA repeat accumulation was prevalent in the cytosol of DM2 patient fibroblasts, facilitating repeat-associated non-AUG translation. The ensuing chronic endoplasmic reticulum (ER) stress response led to an ATF6-controlled induction of type-I IFN dependent on the cGAS/STING pathway. Recapitulating chronic ER stress in the monocytic THP-1 cell line revealed its dependence on mitochondrial DNA (mtDNA). Correspondingly, mitochondrial stress and cytosolic leakage of mtDNA was observed in DM2 patient fibroblasts. Altogether, our study demonstrates a novel mechanism by which large repeat expansions cause

chronic ER and mitochondrial stress and induce a type-I interferon response that predisposes to autoimmunity.

Keywords: ER stress, ATF6, Autoimmunity, type I IFN, repeat expansions

Introduction

Dystrophic myotonia (DM) is the most common form of muscular dystrophy and characterized by autosomal dominant myopathy with myotonia, progressive muscle weakness and multiorgan involvement[1]. Both major types of DM are caused by tri- or tetranucleotide repeat expansions in DNA[2]. Early onset myotonic dystrophy type 1 (DM1) is induced by expanded CTG repeats (>50 repeats) within the 3' untranslated region of the dystrophia myotonica protein kinase (DMPK) gene[3]. At the mRNA level, the expansions of the noncoding CUG repeats result in the formation of stem-loop dsRNA structures that bind and sequester the RNA-binding proteins muscleblind-like 1 (MBNL1) and CUG-binding protein 1 (CUGBP1) preventing their normal function as antagonistic regulators of alternative splicing[4]. MBNL1 sequestration results in fetal isoform expression in adult muscle, a reversion to developmentally inappropriate splicing that leads to muscle dysfunction[5 6].
In contrast, symptoms of myotonic dystrophy type 2 (DM2) usually begin in the second to sixth decade and include proximal muscle weakness, grip myotonia, muscle pain and cataracts[1]. Myotonic dystrophy type 2 is induced by expanded CCTG repeats (>75-11,000 repeats) in intron 1 of cellular nucleic acid-binding protein (CNBP) gene (previously known as zinc finger 9 gene, ZNF9)[7]. In normal individuals, the size of the CCTG repeats in this region is below 30[1]. In DM2, these repeats may expand over the patient's lifetime but usually contract from one generation to the next generation, which might explain the late onset of the disease and the lack of congenital form of the disease[1]. CNBP is an RNA-binding protein that binds G-rich elements in target mRNA coding sequences and supports translation by resolving stable mRNA secondary structures[8,9]. However, a previous report has also not demonstrated an effect of CCUG RNA repeat expansion on expression levels of CNBP protein[10].

Among the complex organ manifestations in DM2, Tieleman et al. described an enhanced frequency of autoimmune diseases and autoantibodies compared with healthy controls and patients with DM1[11]. Increased incidence of autoimmune phenomena in DM2 patients currently lacks a mechanistic explanation. However, the extended RNA expansions in DM2 compared to DM1[12] suggest a direct role for the unrestricted nucleic-acid accumulation in its pathogenesis. It has been shown that CUG and CCUG mRNA repeats can form stable base-paired hairpin structures that translocate from the nucleus to the cytoplasm[13-16]. Disturbances in nucleic acid metabolism have been linked to autoimmune diseases mediated by the induction of type I interferons (IFN)[17]. Prominent examples include hypomorphic variants of DNase or RNase genes, such as the DNase TREX1 or the SKIV2L RNA exosome, which lead to accumulation of nucleic acids in the cytoplasm and the activation of innate immune receptors that induce IFN and pro-inflammatory cytokine release[18]. While activation of the cytosolic dsDNA sensor cGAMP-synthase (cGAS) / Stimulator of Interferon Genes (STING) pathway is central to IFN-driven disease resulting from DNA accumulation, a number of possible innate immune RNA sensors are potentially downstream of accumulated, aberrantly-structured RNA, including TLR3, TLR7, TLR8, PKR, RIG-I and MDA5[19].

In the present study, we show that patients with DM2 have a significantly enhanced risk for development of autoimmune diseases associated with an enhanced type-I IFN-stimulated gene (ISG) signature in blood and tissue. While we did not detect evidence of direct sensing of expanded RNA

repeats by innate RNA sensors in patient cells, we instead observed that RNA and protein repeat expansions induced a cGAS-STING dependent ISG signature. While the expanded RNA repeats cannot directly activate cGAS, their presence was associated with chronically-enhanced endoplasmic reticulum (ER) stress via the ATF6 pathway and associated mitochondrial dysfunction leading to mitochondrial DNA (mtDNA) release and cGAS-STING dependent type-I IFN upregulation. Altogether, our study provides a mechanistic rationale for autoimmune disease in DM2 by linking RNA repeat expansion with ER-mitochondrial stress and the induction of systemic autoinflammation and autoimmunity, with significance for the further study of other RNA repeat-expansion associated diseases.

Results

Enhanced prevalence of autoimmunity in patients with DM2

Driven by the observation of cutaneous autoimmune diseases in patients with DM2, we systematically screened 37 patients with DM2, which revealed an enhanced frequency of autoimmune diseases (40.5%) among these patients compared with the overall prevalence of autoimmune diseases in 5-10% of the general population[20] (Figure 1a). Autoimmune phenomena covered a wide spectrum including morphea, vitiligo, alopecia areata, sicca syndrome, Raynaud's syndrome, rheumatoid arthritis, systemic sclerosis, and type I diabetes (suppl. table 1, suppl. Fig 1). Furthermore, the frequency of antinuclear antibodies was significantly enhanced in patients with DM2 (75.7 %) and in patients with DM1 (61.5 %) compared with a cohort of healthy controls (n=1000) (Figure 1b). Disease-specific antibodies directed against SSA(Ro), centromere, SM/RNP and mitochondrial antigens (AMA) were detected (suppl. table 2).

ISG signature in patients with myotonic dystrophy type 2

In line with the increased prevalence of autoimmune disease, we detected an enhanced type I IFN-stimulated gene (ISG) signature in the blood of DM patients, as calculated by an IFN score[21] of 7 different genes (Figure 1c). Elevated protein levels of the ISG myxovirus resistance protein A (MxA) was detected in lesional skin of patients with DM2 and morphea (Figure 1d). For further analysis, we obtained fibroblasts from skin biopsies of 7 patients with DM2, 4 patients with DM1 and 5 healthy controls for RNA sequencing analysis. Among the 313 genes upregulated in DM2 patients (suppl. table 3), we detected 32 ISGs (Figure 1e). ISG expression was higher in fibroblasts of patients with DM2 compared with DM1 ($p<0.05$,*). Together with the higher prevalence of autoimmunity in DM2 patients (Figure 1a), this demonstrates both a higher prevalence of type I IFN stimulation and autoimmunity in DM2. This finding is supported by the previous report of Tieleman et al.[11], which also observed autoimmune diseases predominantly in DM2 when compared to DM1 and to the general population. Therefore, we concentrated on DM2 for further exploration of the pathogenic mechanisms that could be responsible for ISG upregulation and autoimmunity in those patients. Analysis of IFNβ expression and secretion in fibroblasts of DM2 patients revealed that patient cells maintained an elevated IFN expression in culture that was not detected in the healthy controls (Figure 1f). This chronic type I IFN priming led to elevated IFNβ expression after stimulation with poly (I:C) (Figure 1g). In line with the chronic type I IFN priming, we detected ISG upregulation in cultured DM2 fibroblasts compared with healthy controls (Figure 1h).

Cytosolic RNA repeat accumulation in DM2 fibroblasts

Improper restriction and compartmentalization of nucleic acids acts as a danger signal for the innate immune system and induces type-I IFN signaling[19]. To investigate whether RNA repeats accumulate in the fibroblasts of DM2 patients and in which subcellular compartment(s), we performed RNA fluorescence *in situ* hybridization. Using a GGAC fluorescently labelled probe for detection of CCUG repeats, we detected accumulation of repeat RNA in the nucleus as well as the cytoplasm of DM2 fibroblasts which could be eliminated by RNase treatment and was undetectable in healthy controls (Figure 2a). Quantification of RNA-FISH staining also confirmed that RNA repeats accumulate not only in the nucleus but also in the cytoplasm (Figure 2b).

CNBP expression and function is not impaired in DM2 fibroblasts

Repeat expansion in DM2 affects the first intron of the CNBP gene. In DM2 patient fibroblasts, we saw increased mRNA expression of CNBP, but protein levels were in the normal range (suppl. Fig 2a, b). Since CNBP is involved in the resolution of stable secondary mRNA and DNA structures and binds to G-rich elements[8,9], we compared the number of such G-quadruplex structures in patient cells with healthy controls. G-quadruplex levels were slightly elevated in nuclei of DM2 fibroblasts, which may result from the repeat expansions (suppl. Fig 2c, d). In general, less G-quadruplex structures were detected in the cytoplasm, and there was no difference in G-quadruplex levels between patients and controls (suppl. Fig 2e). These findings suggest that G-quadruplex structures in repeat-RNAs might be continuously controlled in both patients and healthy individuals. G-quadruplex unwinding is mainly done by helicases, in particular ATP-dependent RNA helicase DHX36[8]. To investigate if DHX36 is differently expressed in DM2 patients, we analyzed DHX36 expression levels by RT-PCR. Interestingly, mRNA expression of DHX36 was increased, correlating with the upregulation of CNBP mRNA levels (suppl. Fig 2f, g). However, CNBP and DHX36 protein levels were in the normal range (suppl. Fig 2h).

Cytosolic RNA repeats are not recognized by RNA sensors

Cytoplasmic RNA with specific structures or modifications can be sensed by the innate immune system[22]. The cytosolic sensors retinoic acid inducible gene I (RIG-I) and melanoma differentiation-associated protein 5 (MDA5) recognize short and phosphorylated (5'ppp or 5'pp blunt, base-paired RNA ≥19 bp) or long double-stranded (ds)RNA (>300bp) respectively[22]. Both receptors are broadly expressed and utilize mitochondrial antiviral-signalling protein (MAVS) for their downstream signaling[22]. Toll like receptors (TLR) 3, 7 and 8 recognize RNA in the endosome. While the expression of Toll-like receptor (TLR) 7 and TLR8 is restricted to specific immune cell subsets[19], and there are no reports of their expression in fibroblasts, TLR3 is expressed on the surface and endosome of fibroblasts[22] and could potentially sense RNA released from dying cells into cell culture medium.

To analyze whether RIGI, MDA5, MAVS and TLR3 might contribute to type I IFN induction in patient fibroblasts, we downregulated their expression using siRNA and determined the effect on ISG expression. Although siRNA transfection reduced the levels of all RNA receptors (suppl. Figure 3a-d), we did not observe changes in expression levels of ISGs (Figure 2c-f). To further investigate potential MDA5 activation, we also isolated whole RNA from patient and control cells and transfected it into MDA5-expressing and non-MDA5-expressing Hela cells. Although the positive control high molecular weight poly I:C induced a specific response in MDA5 transfected cells, we did not observe upregulation of CXCL10 after transfection of patient RNA (suppl. Fig 3e). Moreover, cytosolic transfection of DM2 patient-derived RNA into THP1 dual sensor cells did not induce activation of an ISRE reporter (suppl.

Fig 3f), although these cells can respond to RIG-I, MDA5, TLR7 and TLR8 activation. Altogether, our data demonstrate that there is no relevant recognition of RNA repeats by cytosolic and endosomal RNA sensors and no indication for direct RNA sensing as the driver of the type-I IFN response in DM2 fibroblasts.

Another sensor for long dsRNA (>33 base pairs [bp]) or stretches of dsRNA is dsRNA-activated protein kinase (PKR), an RNA restriction factor which upon RNA binding undergoes autophosphorylation and phosphorylates its substrate translation initiation factor eIF2α at serine 51[23,24], thereby inhibiting translation initiation and halting protein synthesis[23]. Western blot analysis of DM2 patient fibroblasts did not show increased phosphorylation of PKR, indicating that RNA repeats are also unlikely to activate the PKR pathway (suppl. Fig 3g).

RAN translation in DM2

Unrestricted RNA repeats can cause a cellular stress response and can be transcribed by repeat associated non-AUG (RAN) translation. It has been reported that in DM2, CCTG and CAGG expansion mutation are bidirectionally transcribed, and the resulting RNAs are RAN translated, producing tetrapeptide expansion proteins with Leu-Pro-Ala-Cys (LPAC) from the sense strand or Gln-Ala-Gly-Arg (QAGR) repeats from the antisense strand[25] (Figure 3a). These proteins were shown to accumulate in DM2 patient brains[25]. Analysis of DM2 fibroblasts revealed accumulation of LPAC proteins in patient fibroblasts by western blot (Figure 3b). The sensitivity of the method was not sufficient to quantify QAGR proteins. However using the previously by Zu et al.[25] established and validated antibodies QAGR as well as LPAC proteins were detected in skin biopsies from DM2 patients with morphea (Figure 3c,d). To investigate possible cellular consequences of accumulating RAN proteins and RNA repeats, we next analyzed the cellular stress response.

Chronic activation of the ER Stress response in DM2 fibroblasts

During cell culture, we observed that patient fibroblasts grew significantly more slowly compared with the fibroblasts of healthy controls (Figure 4a) and exhibited a stronger formation of reactive oxygen species (ROS), indicative of cellular stress (Figure 4b). Further unbiased analysis of RNAseq data revealed activation of genes involved in protein processing in the ER, indicating a possible stress response (Figure 4c). Accumulation of RNA repeats and nonsense proteins can cause cellular toxicity and induce ER stress[26,27]. A stressed ER aims to overcome the disturbance in its homeostasis by activating a complex set of signaling pathways together representing the UPR signaling. The UPR involves a multifaceted interaction between three main signaling pathways, each of which is activated by a different ER-sessile sensor of ER stress, i.e., pancreatic ER kinase (PKR)-like ER kinase (PERK), inositol requiring enzyme 1 (IRE1), and activating transcription factor 6 (ATF6)[28]. The sensors remain in an inactive conformation enforced by the direct binding of the chaperone 78 kDa glucose-regulated protein (GRP78 or BiP) to their luminal domains under homeostatic conditions. If BiP is released due to binding of accumulating unfolded or misfolded proteins, the UPR pathways are activated[28] (Figure 4d).

In patient fibroblasts, we detected an increased mRNA expression of BiP (Figure 4e), that is in line with the previously reported increase of BiP mRNA in DM1 muscle fibres[29] and further models of ER stress induced by misfolded proteins[30] Further analysis demonstrated enhanced protein expression of PERK and its target eIF2α. However, there was no phosphorylation of PERK or eIF2α under steady state conditions, although this could be induced in fibroblasts by thapsigargin (TG), an ER stress inductor

used as a positive control (Figure 4f). Since PERK levels were raised in DM2 fibroblasts, we used siRNA to knockdown this gene in DM2 and healthy control fibroblasts (suppl. Fig 4a). While a knockdown of PERK did not decrease ISG mRNA expression (Figure 4g), it did ameliorate the increased ROS levels in DM2 fibroblasts (Figure 4h). This connection of PERK with ROS induction is in line with a previous study demonstrating that PERK is required at ER-mitochondrial contact sites to convey apoptosis after ROS based ER stress[31].

Moreover, patient fibroblasts also demonstrated a reduced expression of IRE1α protein and no increase in splicing of the IRE1α target XBP1, indicating that the IRE1α pathway was not activated in DM2 fibroblasts (Figure 4i, 4j). In contrast, we found increased expression of ATF6 mRNA in patients compared with healthy controls (Figure 4k). Moreover, while protein expression of full-length ATF6 was in the range of healthy control fibroblasts, we detected significantly higher levels of N-terminal cleaved ATF6 in patient fibroblasts (Figure 4l), indicating activation of the ATF6-mediated ER stress pathway. To determine the influence of ATF6 signaling on the patients' fibroblasts, siRNA-mediated downregulation of ATF6 was performed (suppl. Fig 4b). Strikingly, depletion of ATF6 reduced the ISG mRNA levels in DM2 fibroblasts to the level of the healthy controls (Figure 4m), suggesting that the ATF6 pathway is required for ISG upregulation in DM2 fibroblasts.

Although an acute ER stress response would generally result in activation of all three ER-stress pathways[32], chronic ER stress has been reported to induce selective activation of ATF6 accompanied by increased levels of BiP, reduced levels of IRE1α and a lack of IRE1α and PERK signaling[33], in line with our observations in DM2 fibroblasts. We could also confirm these findings using low-dose thapsigargin (0.2nM, 1nM, 5nM) in healthy control fibroblasts over one week. Chronic ER stress induced BiP mRNA expression as did acute ER stress (suppl. Fig 5a). In contrast, XBP1 splicing was strongly activated after acute ER stress but not detectable after chronic stress (Figure 4n). Chronic ER stress also did not induce phosphorylation of PERK (Figure 4p). However, ATF6 mRNA expression was increased by chronic ER stress, and ATF6 protein was cleaved in response to chronic thapsigargin stimulation in fibroblasts (Figure 4o,p). These findings confirmed the pattern of chronic ER-stress observed in DM2 patient fibroblasts and link chronic ER stress and ATF6 activation to ISG induction in DM2 patient cells.

Activation of ATF6 mediates ER mitochondrial crosstalk and cGAS dependent ISG induction

In order to further investigate the signalling pathways potentially leading to ISG induction downstream of ER-Stress, we used a monocytic cell line, THP-1, which possesses intact pathways for most known RNA sensors and for which CRISPR/Cas9-genome editing is well established[34]. Initially, we tested whether typical inductors of ER-Stress lead to type-I IFN induction in these cells, including the N-glycosylation inhibitor tunicamycin (TN), the SERCA inhibitors thapsigargin (TG), cyclopiazonic acid (CPA) and 2,5-di-*t*-butyl-1,4-benzohydroquinone (BHQ) (Figure 5a). Induction of the ISG CXCL10 could be observed at the protein level for all compounds, albeit at different optimal concentrations. For further experiments, we used representative concentrations of each compound, for which CXCL10 induction (Figure 5a) was observed.

We then generated THP-1 cells deficient in PERK, ATF6A/B and IRE1α using CRISPR/Cas9 genome editing (suppl. table 4) to determine the ER pathway that is responsible for ISG induction in this model. Here, as well, we could clearly observe that deficiency in IRE1α or PERK did not affect ISG induction, while ATF6A/B deficiency completely ablated the ISG response downstream of ER-Stress (Figure 5b), confirming the finding of ATF6-dependent ISG induction in DM2 fibroblasts. We then investigated which upstream sensor might be responsible for ISG induction, using THP-1 deficient in cGAS, STING,

RIG-I, MAVS and IRF3. For all 4 activators of ER stress, CXCL10 induction was dependent on the DNA sensor cGAS, its downstream adaptor STING and the transcription factor IRF3 but not MAVS or RIG-I, linking DNA sensing with IFN induction downstream of acute ER stress (Figure 5c). We then investigated the effect of ATF6 and STING deficiency on IFNβ resulting from chronic ER Stress, induced by low-dose thapsigargin. Here, as well, STING and ATF6 were critically required for IFNβ induction (Figure 5d). To also investigate non-myeloid cells, we also performed the experiments in the epithelial colon carcinoma cell line HT-29. Although these cells were not amenable to experiments with chronic ER stress (data not shown), under acute ER-Stress conditions, they also demonstrated cGAS and STING-dependent CXCL10 induction (suppl. Fig 4e).

Since ER-stress has been associated with release of mitochondrial DNA (mtDNA)[35], a potential cGAS ligand, albeit in conjunction with activation of the NLRP3 inflammasome[36], we then treated THP-1 cells with ethidium bromide to deplete their mtDNA (suppl. Figure 4f). EtBr-treatment significantly reduced mtDNA in THP-1 and, strikingly, also specifically blunted the type I-IFN response to ER-stress but not to exogenous dsDNA (Figure 5e).

MtDNA release is also a hallmark of apoptosis, both downstream of the UPR and due to other causes, and, at the same time, apoptotic cell death is also known to suppress mtDNA-mediated cGAS/STING activation[37,38]. Thus, we investigated whether caspase-3 activation correlated with type-I IFN induction during ER stress. Using titrated amounts of all 4 ER-stress activators, we could observe that, while high levels of activation could efficiently induce apoptosis, these high levels were no efficient inducers of IFN release (as indicated by STAT1 phosphorylation) (suppl. Fig 5b). In contrast, lower levels of the compounds could induce higher levels of STAT1 activation downstream of IFNAR but did not induce apoptotic cell death (suppl. Fig 5b). Thus, ER-stress induces type-I IFN release at subapoptotic levels which still allow for the release of mtDNA. Accordingly, despite ER stress, DM2 fibroblasts did not show signs of apoptosis, and the rate of cells in subG1 was below 0.5 percent (suppl. Fig 5c).

Mitochondrial DNA release triggers cGAS dependent ISG induction in DM2

To analyze whether this ER-mitochondrial connection is also responsible for ISG induction in DM2, we performed siRNA-mediated knockdown of cGAS and STING in DM2 fibroblasts (suppl. Fig 4c, d). Indeed, after reducing cGAS or STING expression, the IFN score was significantly reduced in patient fibroblasts (Figure 6a, b), indicating that the ISG signature in DM2 is cGAS and STING dependent. As fibroblasts did not survive mtDNA depletion with EtBr (data not shown), we analyzed the mitochondrial membrane potential and activation status of DM2-patient fibroblasts to investigate whether these cells also demonstrate mitochondrial activation. Staining with MitoTracker Red (MTR) and flow cytometric analysis showed reduced mean fluorescence intensity (MFI) in patient fibroblasts compared with healthy controls, indicating a lower membrane potential in patient cells that is characteristic for an uncoupling of the mitochondrial membrane and mitochondrial stress (Figure 6c, d). Although the mitochondrial mass was not significantly different between patient and controls (Figure 6e), a cellular response to mitochondrial stress was reflected by upregulation of genes involved in mitophagy (Figure 6f). We observed an upregulation of the mitochondrial genes MFN and OPA (Figure 6f), which have been shown to convey enhanced mitochondrial oxygen consumption during aging[39]. In line with this, we detected an enhanced senescence rate in DM2 fibroblasts by beta-galactosidase staining compared with age-matched controls (Figure 6g). To investigate the oxygen consumption rate more closely, a seahorse assay was performed. Oxygen consumption was increased both with and without stimulation with Carbonyl cyanide-4 (trifluoromethoxy) phenylhydrazone (FCCP) in DM2 fibroblasts compared

with healthy controls (Figure 6h), and ATP production of mitochondria was enhanced after treatment with oligomycin, an inhibitor of ATP synthase (Figure 6h). To further understand the impact of mitochondrial stress on DM2 fibroblasts the release of mtDNA was monitored. Immunofluorescence staining of DNA, cGAS and mitochondria in patient cells using confocal Airyscan microscopy showed cytosolically localized DNA, in proximity to the mitochondria, which colocalized with the DNA sensor cGAS (Figure 6i,j).

Discussion

Here, we report that patients with myotonic dystrophy have an increased prevalence of concomitant autoimmunity associated with a cGAS/STING-dependent activation of the type I IFN response. First, we demonstrate that type I IFN-stimulated genes are upregulated in blood, lesional skin and isolated fibroblasts of patients with DM and especially DM2. This finding is further substantiated by the increased levels of autoantibodies in patients with DM2 that can be regarded as a first sign of autoimmunity. The prevalence of ANA in DM2 patients was elevated compared to healthy controls and is about twice as high as in the general German population (76% versus 36%, respectively)[40]. Two previous reports either demonstrated autoimmunity in DM2 patients[11] or showed an ISG signature in cataract samples from DM2[41] and thus support the association of DM2 with autoimmunity. The stable expression of ISGs in DM2 fibroblasts in culture in comparison with healthy controls suggested that a cell intrinsic mechanism is responsible for this type I IFN signature.

DM2 has the highest number of RNA repeats among all repeat expansion diseases. The number of repeat expansions ranges from 75 to >11,000 repeats which form stable RNA aggregates in the cell[1,10]. We demonstrated that these RNA repeats not only accumulate in the nucleus but also can be frequently detected in the cytoplasm. This nuclear egress of repeat-expansion RNA has previously been reported in a model using repeat-transfected CHO cells[13] but not yet in patient cells. Unrestricted RNA can act as a danger signal in the cell, yet we did not observe evidence for a direct sensing of repeat RNA by specific RNA sensors of the innate immune system. This could potentially be explained by the fact that this self RNA is fully modified and also lacks the specific structures required for recognition by RIG-I, MDA5 or PKR[22]. However, we did observe that repeat RNA led to RAN translation and accumulation of nonsense proteins in fibroblasts and skin of patients, as previously described in the brain of DM2 patients[25]. These proteins can induce cellular stress which may act as a positive feedback loop and further enhance RAN translation[25,42]. The upregulation of eIF2α and PERK indicates such a possible feedback loop because both factors have been recently shown to support RAN translation of LPAC and QAGR in DM2 as alternative initiation factors[43]. An active RAN translation might also be initiated by the ATP-dependent RNA helicase DHX36, which was upregulated at the mRNA level in patient cells and has been shown to facilitate RAN translation of GGGGCC repeat RNAs in cells of patients with amyotrophic lateral sclerosis[44]. The observed enhanced ATP production by mitochondria in DM2 fibroblasts would support the ATP-dependent function of DHX36.

Repeat accumulation in the cell was associated with a chronic ER stress response in fibroblasts from patients with DM2 characterized by activation of the ATF6 pathway. The IRE1α pathway, which is typically induced by acute ER stress and leads to XBP1 splicing and IRE1α upregulation was not activated, and IRE1α itself was downregulated. Interestingly, it has been shown that ATF6 is involved in the downregulation of the protein IRE1α during sustained ER stress[45]. Upon ER stress, ATF6 traffics from the ER to the Golgi apparatus followed by a sequential cleavage[46]. The cleaved active form acts as a transcription factor of various genes controlling organelle homeostasis beyond ER stress[46]. Embryonic mouse fibroblasts deficient in the ER stress sensor ATF6 showed increased apoptosis and decreased adaptation to prolonged or recurrent stress[47]. Our finding in DM2 fibroblasts was substantiated by demonstrating that chronic stimulation of healthy fibroblasts by thapsigargin also

induced selective ATF6 pathway activation, indicating that chronic and acute ER stress responses differ. Interestingly, chronic ER stress in THP1 cells was associated with a similarly low-level type I IFN response as observed in DM2 fibroblasts and, most importantly, in both cell types, the ISG response was dependent on ATF6. These findings demonstrate that chronic ER stress can lead to ATF6-dependent ISG upregulation in fibroblasts and myeloid cells.

The ER is closely connected with mitochondria and physical interactions between these organelles maintain mitochondria-ER contact sites[46]. The UPR member PERK is part of the mitochondria associated ER-membrane and upregulation of this protein in DM2 fibroblasts might be relevant for stabilizing these connections[31,46]. Interestingly, we found that depletion of mitochondrial DNA (mtDNA) completely abrogated the ISG response in THP1 cells, indicating that the ER-mitochondrial connection is required for ISG induction. It has been previously established that mitochondrial stress engages cytosolic antiviral signaling to enhance the expression of a subset of ISGs[48,49]. Aberrant mtDNA packaging promotes escape of mtDNA into the cytosol, where it engages the DNA sensor cGAS and promotes STING dependent ISG upregulation if not inhibited by apoptotic caspases[48]. Our data demonstrate that uncoupling of the mitochondrial membrane chain in response to stress can explain mitochondrial DNA release that can engage cGAS signaling without triggering fulminant apoptosis which would inhibit this pathway[50]. Altogether, these data demonstrate that enabled by the anti-apoptotic effect of the ATF6 pathway chronic ER stress can lead to mitochondria-dependent cGAS/STING induced ISG upregulation.

Chronic, low-level activation of the ISG response in cells of DM2 patients likely promotes the manifestation of autoimmune diseases. We know that autoimmunity can be induced by chronic low-level ISG induction in monogenic interferonopathies caused by mutations that impair intracellular restriction of nucleic acids[17]. For example, familial chilblain lupus is caused by loss-of-function mutations in the DNase TREX1[51,52] which induce accumulation of DNA in the cytoplasm that is sensed by the cGAS-STING-pathway and leads to chronic low level ISG upregulation[53]. Trigger factors such as UV-irradiation or cold exposure enhance the type I IFN response and elucidate diseases flares[54]. Similarly, SLE is promoted by mutations in RNASEH2 that impair ribonucleotide excision from DNA and cause DNA damage and repair-associated chronic ISG upregulation[55]. Thus, our findings place DM2 among other autoimmune diseases manifesting due to cGAS/STING induced chronic ISG upregulation and autoimmunity and into the larger context of type-I interferon driven disease.

In conclusion, we provide evidence for a new disease pathway that connects ATF6 controlled ER Stress in DM2 fibroblasts with mitochondrial DNA release and ISG upregulation (Figure 7). Elucidating this pathway opens new avenues for understanding other illnesses, both monogenetic and multifactorial, that are accompanied by increased ER stress. For instance, ER stress plays a role in the elevated production of ISGs after PRR sensing[28]. In addition, a proinflammatory western diet has been associated with both ER stress and ISG upregulation although these phenomena have not been linked mechanistically to date[56,57]. Furthermore, thapsigargin-induced ER stress has recently been proposed for the treatment of coronavirus infections[58], and ATF6-dependent type-I IFN induction is also likely to be relevant for these reported antiviral effects.

Importantly, our data demonstrate that, like other type-I IFN-associated diseases, DM2 is potentially druggable by compounds interfering with type I IFN activation such as Janus kinase inhibitors or IFNAR receptor blockers. Thus, altogether, this study also provides new potential therapeutic approaches to treating the concomitant manifestation of autoimmune diseases in DM2 patients.

Acknowledgments

This work was supported by the Light Microscopy Facility, a Core Facility of the CMCB Technology Platform at TU Dresden. We thank Saskia Schmitz for expert technical assistance.

Funding: This work was supported by the Deutsche Forschungsgemeinschaft (DFG, German Research Foundation), grant TRR237 369799452/404458960 to CG, EB, KP, MS, TZ. It was also supported by the Deutsche Forschungsgemeinschaft (DFG, German Research Foundation) under Germany's Excellence Strategy–EXC2151–390873048, of which EB, GH, KP and MS are members. FU received funding from BonnNI (Else-Kröner Fresenius Foundation, University Bonn).

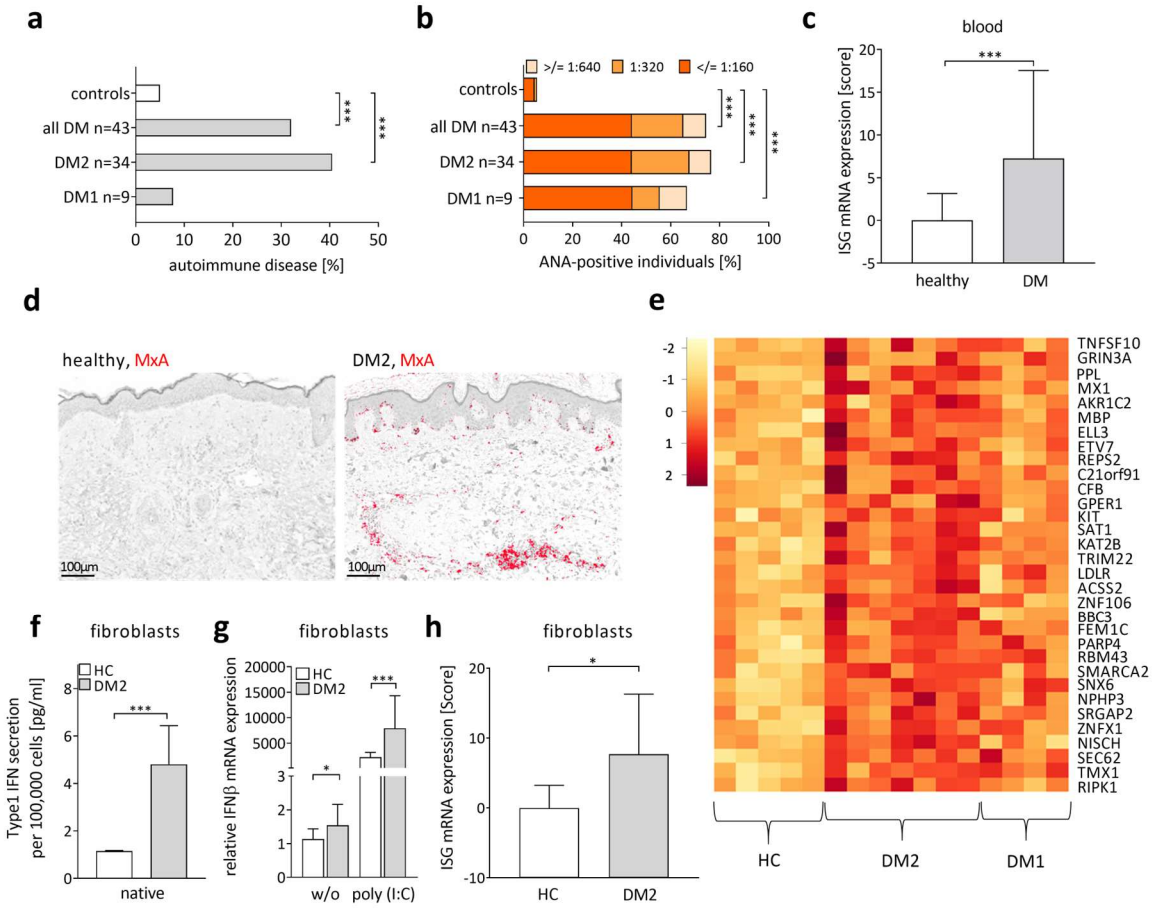

Figure 1: Enhanced type I IFN activation and autoimmunity in patients with myotonic dystrophy. a, frequency of autoimmune diseases among 43 patients with DM (DM1 n=9, DM2 n=34) compared with the frequency of autoimmune diseases in the general population[20] **b**, Antinuclear antibodies (ANA) were determined on Hep-2 cells in the serum of 9 DM1 and 34 DM2 patients compared with data from a control population (n = 1,000) measured in the same laboratory[55]. Shown is the percentage of ANA-positive DM1 and DM2 patients (Mann-Whitney p= 0.001) **c,** calculated IFN score[21] from the blood of 17 healthy controls, 34 DM2 patients and 9 DM1 patients of mRNA expression of the ISGs, IFIT1, IFI44, IFI44L, CXCL10, ISG15, IFI27, and Viperin. **d,** Immunohistochemistry of myxovirus resistance protein A (MxA = red) in 4% formaldehyde-fixed lesional skin sections from a healthy control and a DM2 patient. **e,** Heatmap of ISGs that are significantly increased in 7 DM2 and 4 DM1 fibroblasts cell lines compared to 5 control fibroblasts. Each column represents one cell line. The heatmap depicts log 10 values of z-score. **f**, Determination of type-I IFN expression in the supernatant of 3 control (HC) and 9 DM2 fibroblasts cell lines. **g**, Fibroblasts were treated with 10 µg/ml polyinosinic:polycytidylic acid (Poly I:C), and relative mRNA expression of IFNβ in 3 healthy and 4 DM2 fibroblasts. Relative expression (n-fold) was calculated to the mean of three native healthy controls. **h**, calculated IFN score[21] from 6 healthy control (HC) and 9 DM2 fibroblasts using mRNA expression of the ISGs, IFI44, IFI27, ISG15, Viperin, IFI16, IRF7, TLR3. f-h show data of at least three independent experiments, *=p<0.05, **=p<0.01, ***=p<0.001; f depict mean ± SEM. c,g,h show mean ± SD.

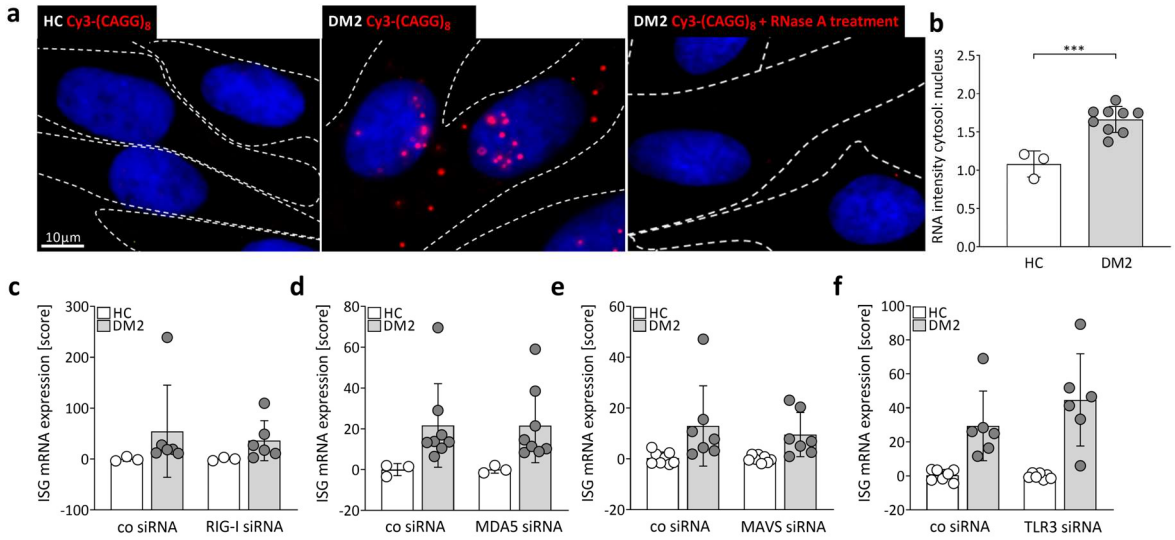

Figure 2: Accumulation of RNA-Repeats in the nucleus and the cytoplasm in DM2 fibroblasts. a, Fluorescence In Situ Hybridization (FISH) of RNA Repeats in fibroblasts. Shown is a representative labeling with the CAGG probe (red) and nuclear staining by DAPI (blue) in one control and one DM2 patient. Pretreatment with 0.5 mg/ml RNase A completely resolved the staining. **b**, Ratio of nuclear versus cytoplasmatic integrated intensity of RNA FISH staining in DM2 patients. **c-f,** calculated IFN score[21] using mRNA expression of 4 ISGs (IFI44, IFI27, IRF7, Viperin) after siRNA knockdown of RIG-I (**e**), MDA5 (**f**), MAVS (**g**) or TLR3 (**h**). a,b, are representative of three independent experiments. c-f, include data from three (c,d), four (f) or six (e) independent experiments. All bars depict mean ± SD, *=p<0.05, **=p<0.01

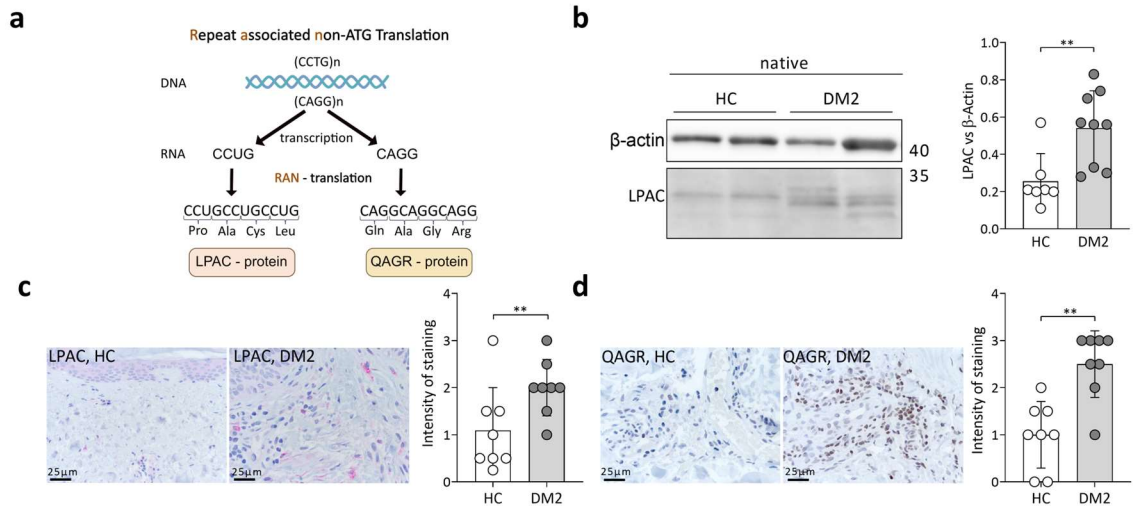

Figure 3: RAN translation in DM2 fibroblasts. a, Schematic representation of the repeat associated non-ATG (RAN) Translation. **b**, protein concentration of LPAC in DM2 and control fibroblasts was determined by western blotting. **c**,**d** Immunohistochemistry (IHC) showing LPAC (red) and QAGR (brown) immunostaining in skin section in healthy control (n = 8) and DM2 (n=7) patients. b, is representative for 9 DM2 patients. c-d, include data from least three (d) independent experiments. All bars depict mean ± SD, *=p<0.05, **=p<0.01, ***=p<0.001;

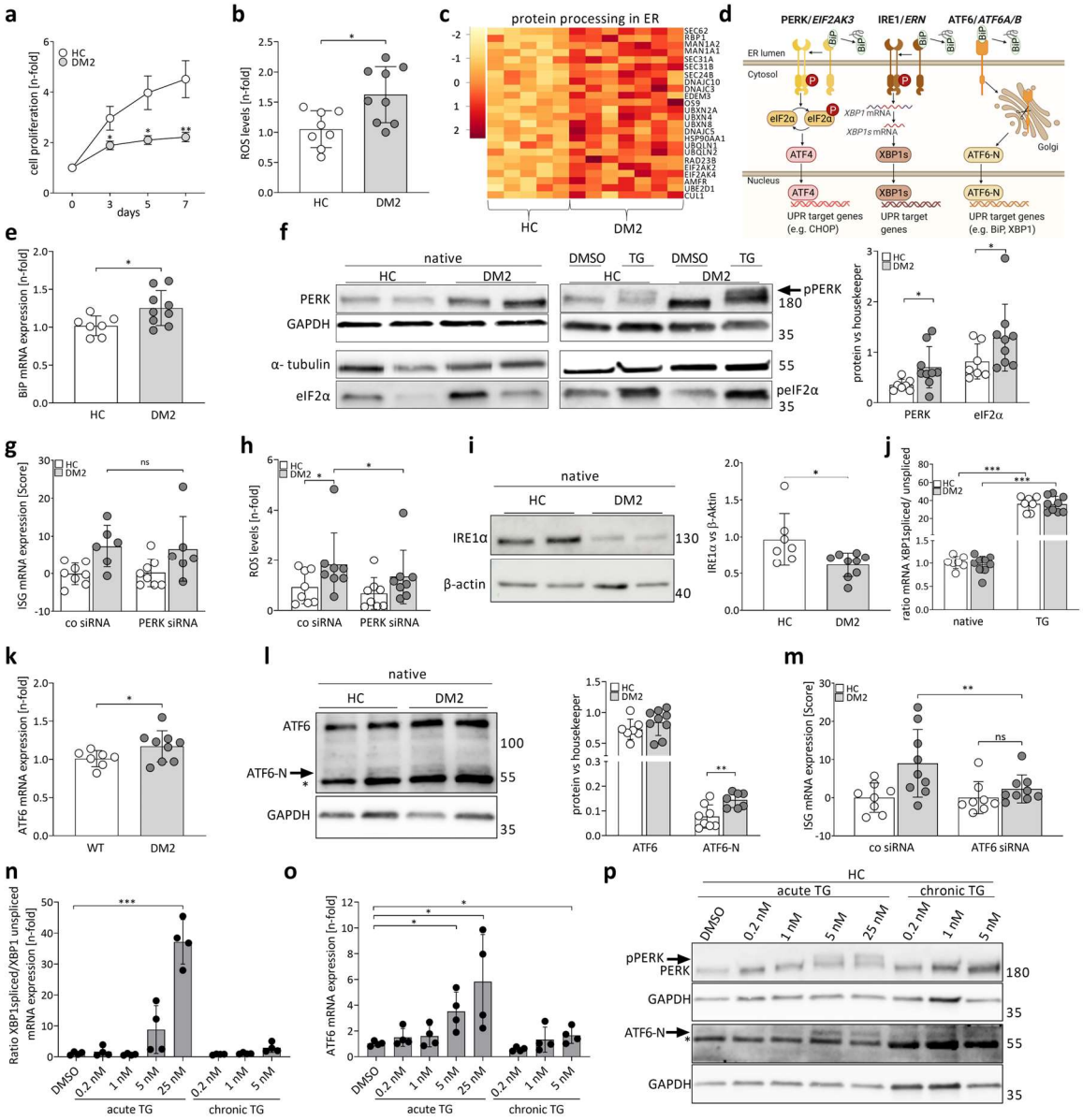

Figure 4: Chronic activation of the ER Stress response in DM2 fibroblasts. a, Proliferation of fibroblasts was measured by staining the DNA with Hoechst 33258 at four different time points (day 0, day 3, day 5, day 7) in 8 fibroblasts controls and 9 DM2 patients. **b**, ROS levels of 9 DM2 patient fibroblasts relative to 8 controls. **c,** RNAseq analysis of 6 DM2 and 5 control fibroblast cell lines reveals significant upregulation of genes from the KEGG pathway "Protein processing in ER". The heatmap depicts log 10 values of z-score. **d**, Schematic representation of the unfolded protein response (UPR). **e,** relative mRNA expression of ER stress factor BiP in 8 controls (HC) and 9 DM2 fibroblasts. **f**, Representative western blot analysis of ER stress factor PERK and eIF2α in fibroblasts of 9 DM2 patients or 7 healthy controls under native conditions (left) and after stimulation with thapsigargin (TG, 50nM), right. **g**, calculated IFN score[21] using mRNA expression of the ISGs IFI44, DDX58, IRF7, Viperin, and Mx1 in fibroblasts after siRNA knockdown of PERK (DM2: n= 6, HC: n=8). **h**, Analysis of ROS levels in 9 DM2 fibroblasts and 8 controls after siRNA knockdown of PERK. **i**, Representative western blot analysis of ER stress factor IRE1α in fibroblasts of 9 DM2 patients or 8 healthy controls under native conditions. **j**, Ratio of unspliced and spliced XBP1 relative mRNA expression under native conditions and after TG (50nM) stimulation in 8 controls and 9 DM2 patients. **k**, relative mRNA expression of ER stress sensor ATF6 in 8 controls (HC) and 9 DM2 fibroblasts. **l**, Representative western blot analysis of ER stress factor

ATF6 (DM2: n=9, HC: n=8) and ATF6-N (DM2: n= 7, HC: n=8) in fibroblasts under native conditions. A nonspecific band is indicated with *. **m**, calculated IFN score[21] using mRNA expression of the ISGs IFI44, DDX58, IRF7, Viperin, and Mx1 in fibroblasts after siRNA knockdown of ATF6. (DM2: n= 9, HC: n=8). **n**, relative mRNA expression of ER stress factors XBP1 (**n**) and ATF6 (**o**) in fibroblasts. To induce acute ER stress, fibroblasts were treated once with 25 nM, 1nM, 5nM and 0.2nM TG. For chronic ER stress, fibroblasts were treated with 5nM, 1nM or 0.2nM TG for one week. **p**, Representative western blot analysis of ER stress factor PERK and ATF6-N in control fibroblasts which were treated with TG to induce acute or chronic ER stress. b,h ROS expression was determined using dihydrorhodamine 123. e,g,i,j,m-o, mRNA expression was determined using RT-PCR. a,b,c-m, include data from three (a,m) or at least three (b, e-l) independent experiments. n-p are representative for 4 healthy donors. a, shows mean ± SEM. b, e-o bars depict mean ± SD , *=p<0.05, **=p<0.01, ***=p<0.001.

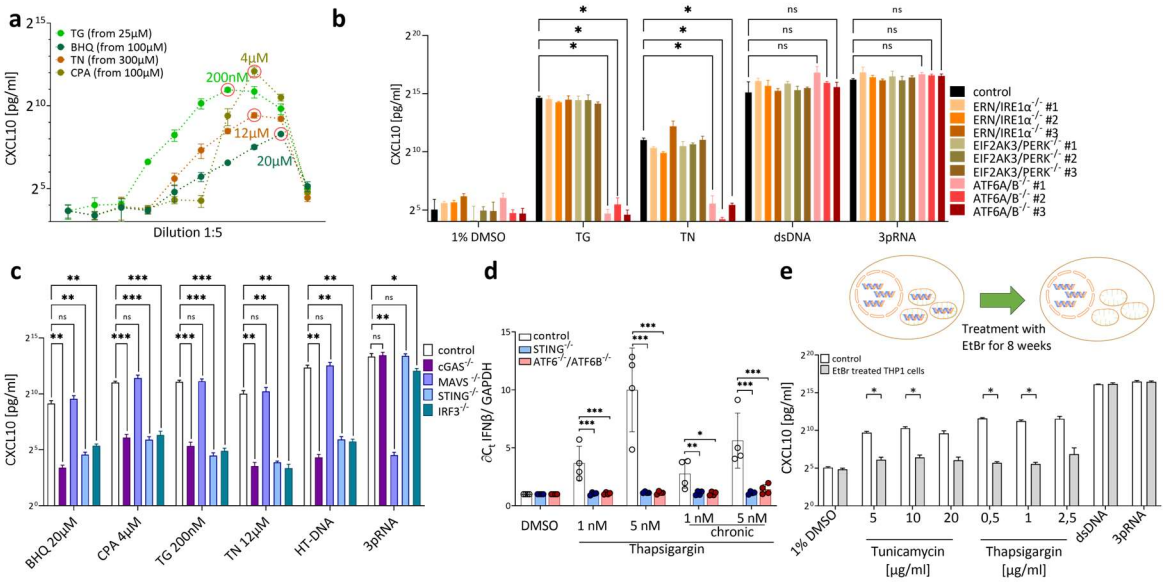

Figure 5: ER stress leads to ATF6 dependent ISG upregulation that depends on sensing of DNA from mitochondria via the cGAS-STING-pathway. a-c, THP1 cells of the indicated genotype were stimulated with the ER-stress inducers cyclopiazonic acid (CPA), 2,5-di-*t*-butyl-1,4-benzohydroquinone (BHQ), thapsigargin (TG) and tunicamycin (TN) at the indicated concentrations or with herring testis (HT)-DNA or 3pRNA. Wildtype THP-1 cells were used in a and as a "control" in b and c. Supernatants were harvested 24h after simulation and probed for CXCL10 levels using ELISA. In a, optimal concentrations for CXCL10 release are circled. **d**, Relative mRNA expression of IFNB in STING$^{-/-}$ and ATF6$^{-/-}$ THP1 cells after acute and chronic ER stress induction. For acute ER stress, THP1 cells were treated once with 1nM and 5nM TG. For chronic ER stress, THP1 cells were treated with 1nM and 5 nM TG for one week. **e**, THP1 cells were treated with EtBr for 8 weeks to deplete mitochondrial DNA. Cells were then stimulated as indicated, and CXCL10 release was determined using ELISA. a-d, show data of three independent experiments, *=p<0.05, **=p<0.01, ***=p<0.001; all error bars represent SD.

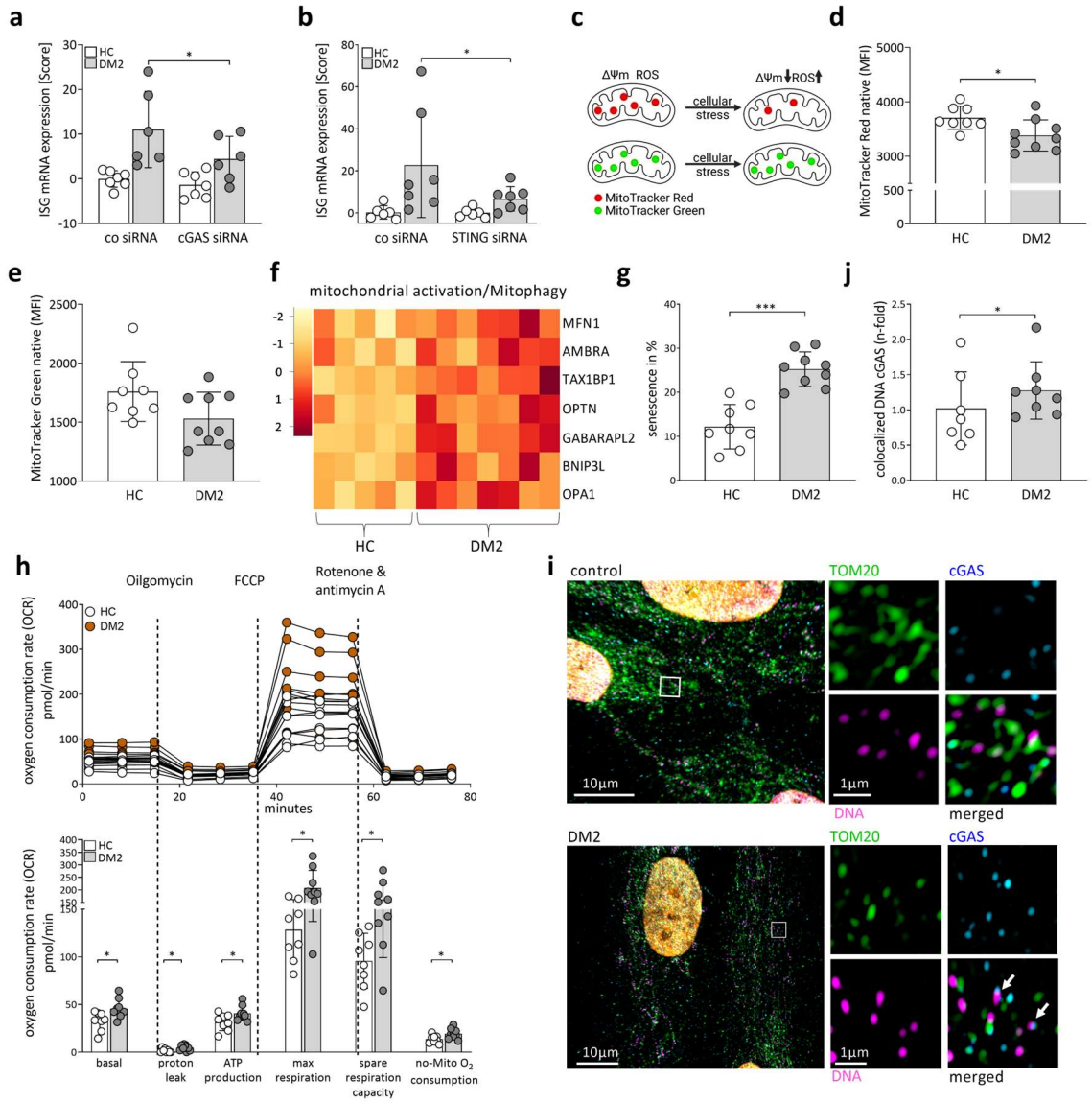

Figure 6: cGAS STING dependent ISG upregulation and mitochondrial stress in fibroblasts of DM2 patients. a, calculated IFN score[21] using mRNA expression of the ISGs IFI44, IRF7, Viperin, Mx1, and DDX58 in the fibroblasts of DM2 patients and healthy controls (HC) after siRNA knockdown of cGAS (DM2 n=6, HC n=7) and STING (**b**, DM2 n=7, HC n=7). **c**, Schematic representation of the function of the MitoTracker red (MTR) and MitoTracker green (MTG). A reduction of membrane potential ΔΨm induced by cell stress leads to reduced uptake of MTR and ROS induction. **d**,**e** fibroblasts of 9 DM2 patients and 8 controls were analyzed by flow cytometry using MTR (**d**) and MTG (**e**). Mean fluorescence intensity (MFI) is shown. **f**, Percentage of senescent cells in fibroblasts cultures from 9 DM2 patients and 8 controls as determined by β-galactosidase assay. **g,** RNAseq analysis in fibroblast of 6 DM2 patients and 5 controls revealed significant upregulation of genes from the KEGG pathway "Mitophagy". The heatmap depicts log 10 values of z-score. **h**, Measurement of oxygen consumption rate (OCR) in fibroblasts from 9 DM2 patients and 8 controls. One representative experiment out of three is shown. **i,** Representative confocal immunofluorescence stainings of mitochondria (TOM20, green), DNA (red) and cGAS (blue) in fibroblasts of DM2 patients and controls. **j**, Quantification of immunofluorescence staining of mitochondria, DNA and cGAS using Arivis Vision 4D 3.5.1 Software. The colocalization between DNA and cGAS outside the mitochondria is shown for 8 DM2 and 7 healthy control (HC) fibroblasts. a, b, mRNA expression was determined using RT-PCR. a,b,d-f, show data of at

least three independent experiments. i,j, representative for 8 DM2 patient, *=p<0.05, **=p<0.01; all bars depict mean ± SD.

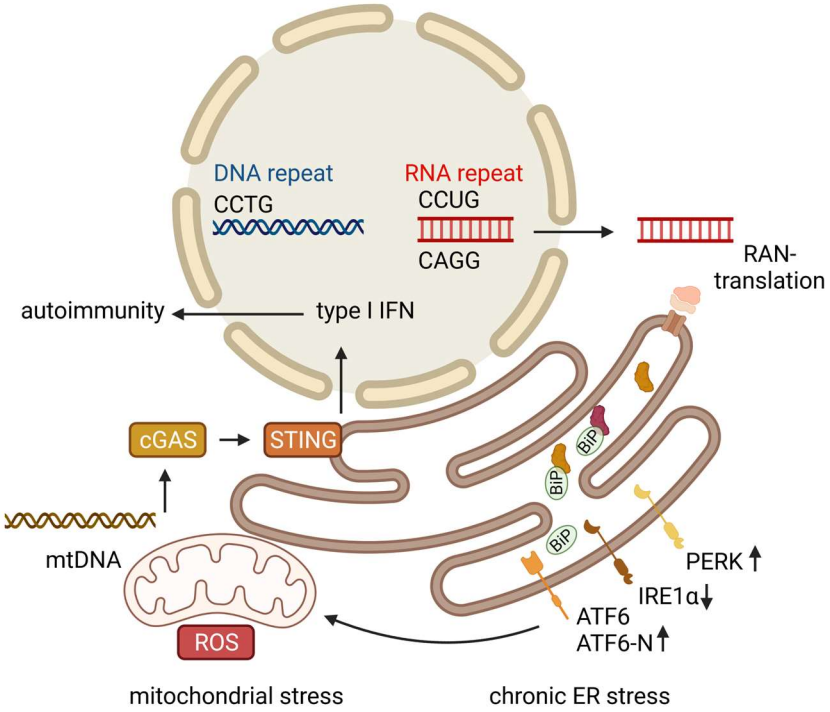

Figure 7: Graphical summary on the proposed mechanism inducing of autoimmunity in DM2. DM2 is characterized by CCTG repeat expansion in DNA that can be transcribed into RNA. RNA repeats accumulate in the nucleus and are transported into the cytoplasm. The cytosolic RNA repeats can be translated by repeat-associated non ATG (RAN) translation. These processes are associated with chronic ER stress indicated by increased BiP, PERK and ATF6-N expression. IRE1α is downregulated, which might be a consequence of ATF6 activation. Depending on ATF6 activation, chronic ER stress leads to mitochondrial activation, DNA release, ROS production and a cGAS-STING dependent upregulation of type I IFN and ISGs. Chronic type I IFN upregulation predisposes to autoimmunity in patients with DM2.

Methods

Patients. Patients with DM2 and DM1 and healthy controls were enrolled after written, informed consent. Human primary fibroblasts were derived from skin biopsies. Control samples were obtained from skin discarded during plastic surgery. The study was approved by the ethics committee of the Medical Faculty, Technische Universität Dresden.

Cell culture and stimulation. Fibroblasts were cultured in DMEM (Gibco) supplemented with 10 % FCS, 1 % antibiotics and 1 mM sodium pyruvate. In all experiments passage-matched cells (passages 6-13) were used. For stimulation of fibroblasts with poly I:C, 10µg/ml (Invivogen #tlrl-pic) was used. Poly I:C was diluted in medium and incubated for 3h. To induce chronic ER stress, fibroblasts were seeded in 6-well plates and incubated with 5nM, 1nM or 0.2 nM thapsigargin (Cayman Chemical Company) for seven days. The medium containing thapsigargin was changed every two days. Acute ER stress was induced in fibroblasts by incubation with 50 nM, 25nM, 5nM, 1nM or 0.2nM thapsigargin for 6h.

THP-1 cells were cultivated in RPMI supplemented with 10 % FCS, 1 % antibiotics and 1 mM sodium pyruvate. dsDNA(1µg/mL) and 3pRNA(200ng/mL) were complexed with Lipofectamine 2000 (Invitrogen) prior to transfection according to the manufacturer's instructions. The ER-stress inducers cyclopiazonic acid (Cayman Chemical Company), 2,5-di-*t*-butyl-1,4-benzohydroquinone (Merck/Sigma-Aldrich), thapsigargin (Cayman Chemical Company) and tunicamycin (Merck/Sigma-Aldrich) were added directly to the cell culture medium at the concentrations indicated in the respective subfigures. Supernatants were harvested for ELISA or RT-PCR 24h after stimulation.

Autoantibody testing. Routine serological tests were carried out at the diagnostic laboratory of the Department of Dermatology and Institute of Immunology, Technische Universität Dresden. ANAs were determined using Hep-2 cells; extractable nuclear antigens were analyzed by immunoblot. Data on ANAs from a reference population were obtained from 1,000 blood donors (samples collected at the Institute of Immunology, Technische Universität Dresden) as described before[55].

RT-PCR. Total RNA from fibroblasts was extracted with the RNeasy Mini Kit (Qiagen) followed by DNase I digestion. Total RNA from blood was extracted with the PAXgene Blood RNA Kit (PreAnalytiX #762174). mRNA expression of DHX36, CNBP, cGAS, STING, RIG-I, MAVS, MDA5, TLR3, IFNβ, ISGs (IFIT1, IFI44, IFI44L, CXCL10, ISG15, IFI27, Viperin, IFI16, IRF7, TLR3, Mx1, DDX58) and ER stress factors (BiP, ATF6, XBP1 spliced, XBP1 unspliced) were determined using iQ SYBR Green Supermix (Bio-Rad #1725124) on an Mx3005P RT-PCR system (Agilent) and normalized to HPRT1. The IFN score was calculated as described by Kirou et al.[21]

Cytokine detection. IFNβ secreted to the supernatants of fibroblasts was quantified using the HEK-Blue™ IFN-α/β reporter system by InvivoGen and normalized to the cell number. Cell number was determined by Hoechst 33258 staining. CXCL10 release was measured using the human IP10 ELISA set (BD Bioscience), performed according to the manufacturer's instructions.

Western blotting. Fibroblasts were lysed in 2x Laemmli buffer (125m M Tris/HCl, pH6.8, 4% SDS, 10% glycerol, 0.02% Bromophenol blue) or RIPA buffer (50 mM Tris-HCl, pH 7.4, 150 mM NaCl, 1 mM EDTA, 1% Triton X-100, 1 mM sodium orthovanadate, 20 mM sodium fluoride) supplemented with 1× Complete Protease Inhibitor Cocktail (Roche) and 1× PhosSTOP phosphatase inhibitors (Roche). THP-1 cells were lysed using 1x Laemmli buffer. 20 µg total protein was subjected to SDS-PAGE electrophoresis followed by Western blotting using antibodies against PKR (Cell Signaling #12297), phospho-STAT1 (Cell Signaling #9167) and cleaved caspase 3 (Cell Signaling #9661), pPKR (Abcam ab32036), LPAC (Merck ABN2258), QAGR (Merck ABN2271), PERK (Cell Signaling #5683) ATF6 (Cell Signaling #65880), ATF6-N (Novus biologicals 75478), IRE1α (Cell Signaling #3294), eIF2α (Cell Signaling #9722), CNBP (Sigma SAB2100453), DHX36 (santa cruz sc-377485) and GAPDH (Cell Signaling #2118), β-actin (Cell Signaling #4970), α-Tubulin (Neomarker MS-581-P1). Immunoreactive signals were detected by chemiluminescence (Super Signal West or Super Signal Pico; Thermo Scientific) Images were taken on Image Quant LAS 4000 (GE Healthcare)

Immunohistochemistry. Paraffin-embedded skin biopsies were cut into 2 to 5-µm sections, rehydrated, and boiled in sodium citrate buffer (pH 6.0). Sections were stained with mouse anti-MxA (provided by O. Haller, Freiburg University, Breisgau, Germany; 1:400 dilution) followed by staining with EnVision G|2 System/AP Rabbit/Mouse (Dako) or antibodies against LPAC (Merck ABN2258) and QAGR (Merck ABN2271). Sections were counterstained with Mayer's hematoxylin (Merck).

Analysis of RNA-Sequencing data. Within the framework of the bioinformatic workflow, raw reads were inspected using fastqc (https://www.bioinformatics.babraham.ac.uk/projects/fastqc/), trimmed using trimmomatic (https://academic.oup.com/bioinformatics/article/30/15/2114/2390096?login=true) and aligned using STAR (https://academic.oup.com/bioinformatics/article/29/1/15/272537?login=true), GRCh37 was used as reference genome. Read counts were extracted from the alignments using the featureCounts method of the subread package (https://academic.oup.com/bioinformatics/article/30/7/923/232889), afterwards DESeq2 was applied to identify differentially expressed genes (https://genomebiology.biomedcentral.com/articles/10.1186/s13059-014-0550-8). Only genes with multiple testing adjusted p-values (padj from DESeq2) < 0.05 were considered significant. The Interferome database was used to identify ISGs[59]. Heatmaps were created using RStudio with the plugin heatmap.2. Data were submitted to National Center for Biotechnology Information (NCBI) under Bioproject ID SUB11601756.

siRNA transfection. Fibroblasts were transfected with 10 nM of RIG-I (Invitrogen 10620319-360113), MDA5 (Invitrogen 10620319-348588), MAVS (Invitrogen 10620319-361473), TLR3 (Invitrogen 10620319-367493), STING (Invitrogen 10620319-361473), cGAS (Invitrogen 10620319-383441), PERK (Invitrogen 21255167) or ATF6 (Invitrogen 10620319-439921) siRNAs. According to the guanine content of the individual siRNAs, the cells were transfected with medium or high control siRNAs (Invitrogen) using Lipofectamine®2000 or Lipofectamine® RNAiMAX (Invitrogen). Cells were prepared 72h after transfection for RT-PCR.

Proliferation. Seeding was done simultaneously for four different time points (day 0, 3, 5, 7). The cells were incubated at 37 °C until the specific time point and then fixed with 4% formaldehyde for 10 minutes, followed by a treatment with 0.25 % TritonX-100 for 10 minutes, both at room temperature. Fibroblasts were then treated with Hoechst 33258 (5 µg/ml) for 15 minutes at room temperature before measurement on a microplate fluorometer. The cell number for each well was determined based on a standard curve using set numbers of cells.

β-galactosidase staining. Fibroblasts were synchronized by serum starvation for 24 hours. The detection of senescence was performed with the Senescence Detection Kit from BioVision (Biozol #K320-250). To enable long-term storage at 4 °C, 1 ml of 70 % glycerol was added to the cells. The plates were analyzed under a light microscope. For each well, four areas were defined, and the blue stained and non-stained cells were counted manually.

MitoTracker staining. To detect mitochondrial stress, 100.000 fibroblasts were incubated for 30 minutes at 37 °C with MitoTracker™ Red FM (200 nM, Invitrogen M22425) and MitoTracker™ Green FM (25 nM, Invitrogen M7514). After incubation, the staining was analyzed by flow cytometry on a FACS Canto II instrument. The analysis of the data was performed using FlowJo software.

ROS detection. For detection of ROS cells were incubated with dihydrorhodamine 123 (DHR 123, Molecular Probes, 1 µg/ml, ChemCruz sc-203027) in DMEM without phenol red. After incubation for 15 minutes at 37 °C, ROS-induced fluorescence was measured on a Tecan microplate reader (excitation 488 nm, emission 530 nm).

Immunofluorescence staining. Fibroblasts were fixed with 4% formaldehyde for 10 minutes at room temperature, followed by permeabilization of the membrane using PBS containing 0.1% Triton X-100. After treatment of the cells with blocking buffer (5% normal goat serum and 0.3% Triton X-100 in 1x PBS), the fibroblasts were incubated with the primary antibody (TOMM20 Abnova #H00009804, 1:1000; anti DNA Progen #61014, 1:100; cGAS Novus Biologicals #NBP1-86761, 1:50) for 2 hours at room temperature, followed by incubation with the appropriate secondary antibody (goat anti-mouse IgM -AF647 (LifeTechnologies, #A-21238); goat anti-rabbit IgG-AF488 (LifeTechnologies, #A-11008); goat anti-mouse IgG1-AF546 (LifeTechnologies, #A-21123)) for 1 hour at room temperature. The images of the fibroblasts were taken with the confocal LSM980/MP. The 63x oil objective was used and a Z-stack was recorded. Images of patients and healthy controls were analyzed using a pipeline created with the Arivis Vision 4D 3.5.1 Software.

RNA-FISH. Cells were seeded in a 24-well plate. Fibroblasts were fixed with 3.7% formaldehyde. Permeabilization was performed using 70% ethanol. RNase A (Thermo Scientific, #EN0531) treatment followed for 1 hour at room temperature. Hybridization of the (CAGG)8 (Eurofine) probe was then performed at 37 °C overnight. Cells were mounted in antifade medium containing DAPI (Thermo Scientific). Cells were imaged using Perkin Elmer Operetta System. The imaging settings were 4 planes per position (DAPI, GFP, mCherry), 40x 0.95 NA objective. Images were then analyzed using the software Cellprofiler (version 3.1.8).

Seahorse Assay. Oxygen consumption rate (OCR) was measured in fibroblasts with Seahorse XFe96 Analyzer (Agilent Technologies) using Seahorse XF Cell Mito Stress Test Kit (103015-100). Fibroblasts (1.5×10^4) were seeded in Agilent Seahorse XF96 cell culture microplates. The assay was carried out in assay medium containing 1mN pyruvate, 2mM glutamine and 10 mM glucose. The modulators used were Oligomycin (2.5 µM), Carbonyl cyanide-4 (trifluoromethoxy) phenylhydrazone (FCCP, 1.0 µM), Rotenone (0.5 µM) and Antimycin (0.5 µM).

CRISPR/Cas9: ATF6A, ATF6B, cGAS, EIF2AK3, ERN1, IRF3, MAVS and STING gRNAs (suppl. table 4) were selected with the CRISPR design tool (Zhang Lab, MIT, crispr.mit.edu) and introduced into an EF1a-Cas9-U6-sgRNA expression plasmid via Gibson assembly. Single-cell clones were obtained by limiting dilution plating; loss of expression was confirmed by immunoblot, and InDels were determined by Sanger sequencing (suppl. table 4). The cGAS and MAVS deficient THP-1 clones have been published previously[60].

mtDNA-depletion/ρ-zero THP1 cells: mitochondrial DNA (mtDNA) was depleted by incubation of wild type (WT) THP1 cells with 50 ng/ml of Ethidium Bromide (EtBr) in standard cell culture medium as described in Widdrington et al.[36]. After four weeks, mtDNA depletion was assessed using RT-PCR for B2M and MT-ND1, which were used as reference genes for nuclear DNA and mtDNA, respectively.

Statistical Analysis. Data are presented as mean ± SD and representative of at least three independent experiments unless otherwise was indicated. Statistical analysis was performed using Graphpad prism version 9.3.1. The normality of distributions was tested using the Shapiro Wilk test. In normally distributed samples, two-tailed Student's t-test was used for comparison of two groups. Samples that were not normally distributed were analyzed by Mann Whitney U test for comparison of two groups. p-values < 0.05 were considered statistically significant. Stars indicate levels of significance: *, ** and *** correspond to $p < 0.05$, $p < 0.01$ and $p < 0.001$, respectively. Images were created with BioRender.com.

References

1. Meola, G. & Cardani, R. Myotonic Dystrophy Type 2: An Update on Clinical Aspects, Genetic and Pathomolecular Mechanism. *J Neuromuscul Dis* **2**, S59-S71 (2015).
2. Jain, A. & Vale, R.D. RNA phase transitions in repeat expansion disorders. *Nature* **546**, 243-247 (2017).
3. Brook, J.D.*, et al.* Molecular basis of myotonic dystrophy: expansion of a trinucleotide (CTG) repeat at the 3' end of a transcript encoding a protein kinase family member. *Cell* **68**, 799-808 (1992).
4. Miller, J.W.*, et al.* Recruitment of human muscleblind proteins to (CUG)(n) expansions associated with myotonic dystrophy. *EMBO J* **19**, 4439-4448 (2000).
5. Lin, X.*, et al.* Failure of MBNL1-dependent post-natal splicing transitions in myotonic dystrophy. *Hum Mol Genet* **15**, 2087-2097 (2006).
6. Wheeler, T.M. & Thornton, C.A. Myotonic dystrophy: RNA-mediated muscle disease. *Curr. Opin. Neurol* **20**, 572-576 (2007).
7. Liquori, C.L.*, et al.* Myotonic dystrophy type 2 caused by a CCTG expansion in intron 1 of ZNF9. *Science* **293**, 864-867 (2001).
8. Sauer, M.*, et al.* DHX36 prevents the accumulation of translationally inactive mRNAs with G4-structures in untranslated regions. *Nat Commun* **10**, 2421 (2019).
9. Benhalevy, D.*, et al.* The Human CCHC-type Zinc Finger Nucleic Acid-Binding Protein Binds G-Rich Elements in Target mRNA Coding Sequences and Promotes Translation. *Cell Rep* **18**, 2979-2990 (2017).
10. Margolis, J.M., Schoser, B.G., Moseley, M.L., Day, J.W. & Ranum, L.P. DM2 intronic expansions: evidence for CCUG accumulation without flanking sequence or effects on ZNF9 mRNA processing or protein expression. *Hum Mol Genet* **15**, 1808-1815 (2006).
11. Tieleman, A.A., den Broeder, A.A., van de Logt, A.E. & van Engelen, B.G. Strong association between myotonic dystrophy type 2 and autoimmune diseases. *J. Neurol. Neurosurg. Psychiatry* **80**, 1293-1295 (2009).
12. Mankodi, A.*, et al.* Ribonuclear inclusions in skeletal muscle in myotonic dystrophy types 1 and 2. *Ann Neurol* **54**, 760-768 (2003).
13. Jones, K.*, et al.* RNA Foci, CUGBP1, and ZNF9 are the primary targets of the mutant CUG and CCUG repeats expanded in myotonic dystrophies type 1 and type 2. *Am J Pathol* **179**, 2475-2489 (2011).
14. Mooers, B.H., Logue, J.S. & Berglund, J.A. The structural basis of myotonic dystrophy from the crystal structure of CUG repeats. *Proc Natl Acad Sci U S A* **102**, 16626-16631 (2005).
15. Dere, R., Napierala, M., Ranum, L.P. & Wells, R.D. Hairpin structure-forming propensity of the (CCTG.CAGG) tetranucleotide repeats contributes to the genetic instability associated with myotonic dystrophy type 2. *J Biol Chem* **279**, 41715-41726 (2004).
16. Jones, K.*, et al.* Reduction of toxic RNAs in myotonic dystrophies type 1 and type 2 by the RNA helicase p68/DDX5. *Proc Natl Acad Sci U S A* **112**, 8041-8045 (2015).
17. Gunther, C. Research in practice: Disturbance in intracellular nucleic acid metabolism promotes lupus erythematosus. *J Dtsch Dermatol Ges* **19**, 209-213 (2021).
18. Lee-Kirsch, M.A. The Type I Interferonopathies. *Annu Rev Med* **68**, 297-315 (2017).
19. Bartok, E. & Hartmann, G. Immune Sensing Mechanisms that Discriminate Self from Altered Self and Foreign Nucleic Acids. *Immunity* **53**, 54-77 (2020).
20. Cooper, G.S., Bynum, M.L. & Somers, E.C. Recent insights in the epidemiology of autoimmune diseases: improved prevalence estimates and understanding of clustering of diseases. *J Autoimmun* **33**, 197-207 (2009).
21. Kirou, K.A.*, et al.* Coordinate overexpression of interferon-alpha-induced genes in systemic lupus erythematosus. *Arthritis Rheum* **50**, 3958-3967 (2004).
22. Schlee, M. & Hartmann, G. Discriminating self from non-self in nucleic acid sensing. *Nat Rev Immunol* **16**, 566-580 (2016).
23. Nallagatla, S.R. & Bevilacqua, P.C. Nucleoside modifications modulate activation of the protein kinase PKR in an RNA structure-specific manner. *RNA* **14**, 1201-1213 (2008).
24. Tian, B.*, et al.* Expanded CUG repeat RNAs form hairpins that activate the double-stranded RNA-dependent protein kinase PKR. *RNA* **6**, 79-87 (2000).
25. Zu, T.*, et al.* RAN Translation Regulated by Muscleblind Proteins in Myotonic Dystrophy Type 2. *Neuron* **95**, 1292-1305.e1295 (2017).
26. Zhang, Y.-J.*, et al.* Aggregation-prone c9FTD/ALS poly(GA) RAN-translated proteins cause neurotoxicity by inducing ER stress. *Acta neuropathologica* **128**, 505-524 (2014).

27. Nguyen, L., Cleary, J.D. & Ranum, L.P.W. Repeat-Associated Non-ATG Translation: Molecular Mechanisms and Contribution to Neurological Disease. *Annu Rev Neurosci* **42**, 227-247 (2019).
28. Sprooten, J. & Garg, A.D. Type I interferons and endoplasmic reticulum stress in health and disease. *Int Rev Cell Mol Biol* **350**, 63-118 (2020).
29. Ikezoe, K.*, et al.* Endoplasmic reticulum stress in myotonic dystrophy type 1 muscle. *Acta Neuropathol* **114**, 527-535 (2007).
30. Kroeger, H.*, et al.* Induction of Endoplasmic Reticulum Stress Genes, BiP and Chop, in Genetic and Environmental Models of Retinal Degeneration. *Investigative Ophthalmology & Visual Science* **53**, 7590-7599 (2012).
31. Verfaillie, T.*, et al.* PERK is required at the ER-mitochondrial contact sites to convey apoptosis after ROS-based ER stress. *Cell Death & Differentiation* **19**, 1880-1891 (2012).
32. Zhang, K. & Kaufman, R.J. From endoplasmic-reticulum stress to the inflammatory response. *Nature* **454**, 455-462 (2008).
33. Casrouge, A.*, et al.* Herpes simplex virus encephalitis in human UNC-93B deficiency. *Science* **314**, 308-312 (2006).
34. Ostendorf, T.*, et al.* Immune Sensing of Synthetic, Bacterial, and Protozoan RNA by Toll-like Receptor 8 Requires Coordinated Processing by RNase T2 and RNase 2. *Immunity* **52**, 591-605.e596 (2020).
35. Bronner, D.N.*, et al.* Endoplasmic Reticulum Stress Activates the Inflammasome via NLRP3- and Caspase-2-Driven Mitochondrial Damage. *Immunity* **43**, 451-462 (2015).
36. Widdrington, J.D.*, et al.* Mitochondrial DNA depletion induces innate immune dysfunction rescued by IFN-γ. *The Journal of allergy and clinical immunology* **140**, 1461-1464.e1468 (2017).
37. Rongvaux, A.*, et al.* Apoptotic caspases prevent the induction of type I interferons by mitochondrial DNA. *Cell* **159**, 1563-1577 (2014).
38. White, M.J.*, et al.* Apoptotic caspases suppress mtDNA-induced STING-mediated type I IFN production. *Cell* **159**, 1549-1562 (2014).
39. Son, J.M.*, et al.* Mitofusin 1 and optic atrophy 1 shift metabolism to mitochondrial respiration during aging. *Aging cell* **16**, 1136-1145 (2017).
40. Akmatov, M.K.*, et al.* Anti-nuclear autoantibodies in the general German population: prevalence and lack of association with selected cardiovascular and metabolic disorders—findings of a multicenter population-based study. *Arthritis Research & Therapy* **19**, 127 (2017).
41. Rhodes, J.D.*, et al.* Activation of the innate immune response and interferon signalling in myotonic dystrophy type 1 and type 2 cataracts. *Hum. Mol. Genet* **21**, 852-862 (2012).
42. Green, K.M.*, et al.* RAN translation at C9orf72-associated repeat expansions is selectively enhanced by the integrated stress response. *Nature Communications* **8**, 2005 (2017).
43. Tusi, S.K.*, et al.* The alternative initiation factor eIF2A plays key role in RAN translation of myotonic dystrophy type 2 CCUG•CAGG repeats. *Hum Mol Genet* **30**, 1020-1029 (2021).
44. Tseng, Y.J.*, et al.* The RNA helicase DHX36-G4R1 modulates C9orf72 GGGGCC hexanucleotide repeat-associated translation. *J Biol Chem* **297**, 100914 (2021).
45. Walter, F., O'Brien, A., Concannon, C.G., Düssmann, H. & Prehn, J.H.M. ER stress signaling has an activating transcription factor 6α (ATF6)-dependent "off-switch". *J Biol Chem* **293**, 18270-18284 (2018).
46. Kumar, V. & Maity, S. ER Stress-Sensor Proteins and ER-Mitochondrial Crosstalk-Signaling Beyond (ER) Stress Response. *Biomolecules* **11**(2021).
47. Wu, J.*, et al.* ATF6alpha optimizes long-term endoplasmic reticulum function to protect cells from chronic stress. *Developmental cell* **13**, 351-364 (2007).
48. West, A.P.*, et al.* Mitochondrial DNA stress primes the antiviral innate immune response. *Nature* **520**, 553 (2015).
49. Riley, J.S. & Tait, S.W. Mitochondrial DNA in inflammation and immunity. *EMBO reports* **21**, e49799 (2020).
50. Willemsen, J.*, et al.* TNF leads to mtDNA release and cGAS/STING-dependent interferon responses that support inflammatory arthritis. *Cell Rep* **37**, 109977 (2021).
51. Gunther, C., Berndt, N., Wolf, C. & Lee-Kirsch, M.A. Familial chilblain lupus due to a novel mutation in the exonuclease III domain of 3' repair exonuclease 1 (TREX1). *JAMA Dermatol* **151**, 426-431 (2015).
52. Lee-Kirsch, M.A.*, et al.* A mutation in TREX1 that impairs susceptibility to granzyme A-mediated cell death underlies familial chilblain lupus. *J Mol. Med* **85**, 531-537 (2007).
53. Wolf, C.*, et al.* RPA and Rad51 constitute a cell intrinsic mechanism to protect the cytosol from self DNA. *Nat Commun* **7**, 11752 (2016).

54. Berndt, N., *et al.* Photosensitivity and cGAS-Dependent IFN-1 Activation in Patients with Lupus and TREX1 Deficiency. *J Invest Dermatol* **142**, 633-640 e636 (2022).
55. Gunther, C., *et al.* Defective removal of ribonucleotides from DNA promotes systemic autoimmunity. *J. Clin. Invest* **125**, 413-424 (2015).
56. Christ, A., *et al.* Western Diet Triggers NLRP3-Dependent Innate Immune Reprogramming. *Cell* **172**, 162-175.e114 (2018).
57. Kawasaki, N., Asada, R., Saito, A., Kanemoto, S. & Imaizumi, K. Obesity-induced endoplasmic reticulum stress causes chronic inflammation in adipose tissue. *Scientific Reports* **2**, 799 (2012).
58. Shaban, M.S., *et al.* Multi-level inhibition of coronavirus replication by chemical ER stress. *Nat Commun* **12**, 5536 (2021).
59. Rusinova, I., *et al.* Interferome v2.0: an updated database of annotated interferon-regulated genes. *Nucleic Acids Res* **41**, D1040-1046 (2013).
60. Ofir-Birin, Y., *et al.* Malaria parasites both repress host CXCL10 and use it as a cue for growth acceleration. *Nat Commun* **12**, 4851 (2021).
61. Biffi, G., Di Antonio, M., Tannahill, D. & Balasubramanian, S. Visualization and selective chemical targeting of RNA G-quadruplex structures in the cytoplasm of human cells. *Nat Chem* **6**, 75-80 (2014).

Supplementary Files

This is a list of supplementary files associated with this preprint. Click to download.

- Supplements.pdf